Published in final edited form as:
Biochemistry. 2013 January 22; 52(3): 537–546. doi:10.1021/bi301650d.

Catalysis by Orotidine 5′-Monophosphate Decarboxylase: Effect of 5-Fluoro and 4′-Substituents on the Decarboxylation of Two-Part Substrates†

Bogdana Goryanova, **Krisztina Spong**, **Tina L. Amyes**, and **John P. Richard***
Department of Chemistry, University at Buffalo, SUNY, Buffalo, New York 14260-3000

Abstract

The syntheses of two novel truncated analogs of the natural substrate orotidine 5′-monophosphate (**OMP**) for orotidine 5′-monophosphate decarboxylase (OMPDC) with enhanced reactivity towards decarboxylation are reported: 1-(β-D-erythrofuranosyl)-5-fluoroorotic acid (**FEO**) and 5′-deoxy-5-fluoroorotidine (**5′-dFO**). A comparison of the second-order rate constants for the OMPDC-catalyzed decarboxylations of **FEO** (10 M^{-1} s^{-1}) and 1-(β-D-erythrofuranosyl)orotic acid (**EO**, 0.026 M^{-1} s^{-1}) shows that the vinyl carbanion-like transition state is stabilized by 3.5 kcal/mol by interactions with the 5-F substituent of **FEO**. The OMPDC-catalyzed decarboxylations of **FEO** and **EO** are both activated by exogenous phosphite dianion (HPO_3^{2-}), but the 5-F substituent results in only a 0.8 kcal stabilization of the transition state for the phosphite-activated reaction of **FEO**. This provides strong evidence that the phosphite-activated OMPDC-catalyzed reaction of **FEO** is not limited by the chemical step of decarboxylation of the enzyme-bound substrate. Evidence is presented that there is a change in rate-limiting step from the chemical step of decarboxylation for the phosphite-activated reaction of **EO**, to closure of the phosphate gripper loop and an enzyme conformational change at the ternary **E**·**FEO**·HPO_3^{2-} complex for the reaction of **FEO**. The 4′-CH_3 and 4′-CH_2OH groups of **5′-dFO** and orotidine, respectively, result in identical destabilizations of the transition state for the unactivated decarboxylation of 2.9 kcal/mol. By contrast, the 4′-CH_3 group of **5′-dFO** and the 4′-CH_2OH group of orotidine result in very different 4.7 and 8.3 kcal/mol destabilizations of the transition state for the phosphite-activated decarboxylation. Here, the destabilizing effect of the 4′-CH_3 substituent at **5′-dFO** is masked by the rate-limiting conformational change that depresses the third-order rate constant for the phosphite-activated reaction of the parent substrate **FEO**.

Orotidine 5′-monophosphate decarboxylase (OMPDC) employs no metal ions or other cofactors yet effects an enormous 10^{17}-fold acceleration of the decarboxylation of enzyme-bound orotidine 5′-monophosphate (**OMP**, Scheme 1A) to give uridine 5′-monophosphate (**UMP**).[1,2] We have shown that the enzymatic reaction proceeds by a stepwise mechanism through a vinyl carbanion intermediate,[3-6] and the overall rate acceleration corresponds to a 31 kcal/mol stabilization of the transition state by interactions of **OMP** with the protein catalyst.[1,2] The functionalities present in the substrate **OMP** are, in principle, sufficient to account for this large transition state binding energy, but the mechanism for the *increase* in the stabilizing binding interactions with the protein from ca. 8 kcal/mol at the ground state Michaelis complex (K_m = 1.4 μM)[7,8] to 31 kcal/mol at the transition state for decarboxylation is poorly understood.[9,10] This specificity in transition state binding is a feature of enzyme-catalyzed reactions that exhibit large transition state binding energies, and

†This work was supported by Grant GM39754 from the National Institutes of Health

*To whom correspondence should be addressed. *Tel:* (716) 645 4232; *Fax:* (716) 645 6963; jrichard@buffalo.edu.

is required to prevent the irreversible formation of tight Michaelis complexes with the reactant and/or product.

We have developed novel experimental protocols for study of the mechanism of action of OMPDC and have used these to characterize the enzyme specificity in binding the transition state as follows. First, we first characterized the interactions between the phosphodianion group of **OMP** and OMPDC, by evaluating the effect of removal of the 4′-$CH_2OPO_3^{2-}$ group of **OMP** to give the *truncated neutral* substrate 1-(β-D-erythrofuranosyl)orotic acid (**EO**, Scheme 1B). The second-order rate constant for OMPDC-catalyzed decarboxylation of **EO** is 4×10^8-fold smaller than that for **OMP**, which shows that interactions of the protein with the 4′-$CH_2OPO_3^{2-}$ group of **OMP** provide a ca. 12 kcal/mol stabilization of the transition state for decarboxylation.[11] However, these interactions do not simply *anchor* **OMP** to OMPDC, because ca. 8 kcal/mol of this phosphodianion binding energy is recovered as transition state stabilization from the binding of phosphite dianion (HPO_3^{2-}) to the transition state in the *phosphite-activated* decarboxylation of **EO** (Scheme 1B).[7,11-13] The activation of OMPDC by phosphite dianion results from the high specificity of the dianion for binding to the *transition state* for the OMPDC-catalyzed decarboxylation of **EO**, compared with the weak binding of phosphite to the free enzyme ($K_d \approx 0.1$ M).[11] We propose that OMPDC exhibits the same *specificity* for the tethered 4′-$CH_2OPO^{2-}{}_3$ group of **OMP** so that the binding interactions of this substrate moiety are utilized for transition state stabilization.[10,13]

Second, OMPDC was shown to provide effective catalysis of the exchange for deuterium of the C-6 protons of **UMP** and 5-fluorouridine 5′-monophosphate (**FUMP**) in D_2O (Scheme 2A).[3,5,14] The kinetic data for the enzymatic and nonenzymatic deuterium exchange reactions of **UMP** and **FUMP** show that OMPDC stabilizes the vinyl carbanion intermediate relative to the bound substrate by *at least* 13 kcal/mol.[3,5] This strong stabilization of the **UMP** and **FUMP** vinyl carbanion intermediates (Scheme 2A) is reflected in the high *specificity* of OMPDC for binding the carbanion-like transition state of the enzyme-catalyzed deuterium exchange reactions.[15,16]

Third, these protocols were combined in a study of the OMPDC-catalyzed exchange for deuterium of the C-6 proton of the *truncated* substrate 1-(β-D-erythrofuranosyl)-5-fluorouracil (**FEU**) in D_2O (Scheme 2B).[17] The observed activation of this reaction by phosphite dianion shows that there is a large ca. 6 kcal/mol stabilization of the vinyl carbanion-like transition state by interactions with HPO_3^{2-}, which is similar to the ca. 8 kcal/mol stabilization of the transition state for the phosphite-activated decarboxylation of **EO**.[11] We concluded that phosphite dianion exhibits the same high *specificity* for binding to the vinyl carbanion-like transition states that are common to the OMPDC-catalyzed decarboxylation and C-6 deuterium exchange reactions (Schemes 1B and 2B).

The addition of a 5-fluoro substituent to **UMP** to give **FUMP** results in a 3400-fold increase in the rate constant for the OMPDC-catalyzed C-6 deuterium exchange reaction of the enzyme-bound nucleotide in D_2O, as a result of stabilization of the negative charge at the vinyl carbanion intermediate by interaction with the electron-withdrawing 5-F substituent.[3,5] By contrast, the stabilization of the vinyl carbanion-like transition state for the OMPDC-catalyzed decarboxylation of **OMP** by a 5-F substituent is not easily quantified, because the decarboxylation of 5-fluoroorotidine 5′-monophosphate (**FOMP**) is limited by substrate binding (k_{cat}/K_m) or product release (k_{cat}).[18] We report here that the second-order rate constant for the OMPDC-catalyzed decarboxylation of the *novel truncated* substrate 1-(β-D-erythrofuranosyl)-5-fluoroorotic acid (**FEO**, Scheme 1B) is 400-fold larger than that for the decarboxylation of **EO**. Surprisingly, we find that the third-order rate constant for the *phosphite!activated* decarboxylation of **FEO** is only 4-fold larger than that for the

decarboxylation of **EO**. The obliteration of the 5-F substituent effect is attributed to a change in rate-limiting step for the phosphite-activated reaction, from the chemical step of decarboxylation for **EO** to an obligate conformational change for the reaction of **FEO**.

We also report the effect of 4′-substituents on the kinetic parameters for the OMPDC-catalyzed decarboxylation reactions of **EO** and **FEO**. The addition of a 4′-CH_2OH group to **EO** to give orotidine or of a 4′-CH_3 group to **FEO** to give 5′-deoxy-5-fluoroorotidine (**5′-dFO**) results in identical destabilizations of the transition state for OMPDC-catalyzed decarboxylation of 2.9 kcal/mol. These surprisingly large 4′-CH_2OH and 4′-CH_3 substituent effects provide striking evidence that OMPDC-catalyzed decarboxylation proceeds through a transition state that is stabilized by a highly organized, but easily disrupted, network of protein-ligand interactions that extend from the substrate phosphodianion group to the pyrimidine binding loci at OMPDC.

EXPERIMENTAL SECTION

Materials

Orotidine 5′-monophosphate and 1-(β-D-erythrofuranosyl)-5-fluorouracil (**FEU)** were available from our earlier studies.[4,7,17,19] 5′-Deoxy-5-fluorouridine (**5′-dFU**, 98%) was purchased from AK Scientific. Orotidine, 5-fluorouridine (≥ 99.0%), ethyl cyanoformate (99%), diisopropylamine (redistilled, 99.95%), butyllithium (1.6 M solution in hexanes) and 3-(N-morpholino)propanesulfonic acid (MOPS, ≥ 99.5%) were purchased from Sigma-Aldrich. Sodium phosphite (dibasic, pentahydrate) was purchased from Riedel-de Haën (Fluka). Acetone was dried over calcium sulfate ($CaSO_4$) and distilled prior to use. Water was from a Milli-Q Academic purification system. All other chemicals were reagent grade or better and were used without further purification.

Wildtype orotidine 5′-monophosphate decarboxylase from *Saccharomyces cerevisiae* (OMPDC) was prepared as described previously.[12,18] The protein sequence differs from the published sequence for wildtype yeast OMPDC by the following mutations: S2H, C155S, A160S and N267D.[12,18] The C155S mutation does not affect the kinetic parameters or the overall structure of the enzyme.[20]

Chemical Syntheses

Our syntheses of the novel compounds 1-(β-D-erythrofuranosyl)-5-fluoroorotic acid (**FEO**) and 5′-deoxy-5-fluoroorotidine (**5′-dFO**) are summarized in Scheme 3. Lithium diisopropylamide (LDA) was prepared from redistilled diisopropylamine and butyllithium (BuLi, 1.6 M solution in hexanes) by the following procedure: BuLi (2 mL, 3.2 mmol) was added slowly to a solution of diisopropylamine (0.5 mL, 3.6 mmol) in dry tetrahydrofuran (THF, 30 mL) under argon at −78 °C. The solution was stirred under argon for 1 h at −78 °C and the whole was used immediately as described below.

^1H and ^{19}F NMR spectra were acquired on a Varian Unity Inova 500 spectrometer operating at 500 MHz for proton. Proton chemical shifts (δ ppm) were referenced to the appropriate solvent peak: 4.69 ppm for HOD in D_2O, 2.54 ppm for d_5-DMSO in d_6-DMSO, and 7.26 ppm for $CHCl_3$ in $CDCl_3$. Proton chemical shift assignments were confirmed using two-dimensional ^1H-^1H correlated spectroscopy (^1H-^1H COSY).

2′,3′-O-Isopropylidene-1-(β-D-erythrofuranosyl)-5-fluorouracil (1a)—The ribosyl hydroxyl groups of **FEU** and **5′-dFU** were protected using adaptations of published procedures as follows.[21] **FEU** (0.31 g, 1.34 mmol) was dried *in vacuo* over activated molecular sieves (4 Å) for 24 h at 50 °C and then dissolved in dry acetone (22 mL). The

reaction was initiated by the slow addition of concentrated H_2SO_4 (0.16 mL) under argon at 0 °C. After 80 min at room temperature the solution was poured into saturated aqueous $NaHCO_3$ (10 mL), stirred for 25 min at room temperature, and extracted with chloroform (4 × 30 mL). The combined organic extracts were dried ($MgSO_4$) and the solvent was removed by evaporation under reduced pressure to give **1a** as a white solid (0.34 g, 1.25 mmol, 93%) which was used without further purification. ^{1}H NMR (500 MHz, $CDCl_3$) δ ppm: 9.16 (s, 1H, NH), 7.34 (d, 1H, J_{HF} = 6 Hz, C6-H), 5.39 (broad s, 1H, C1′-H), 5.18 (d, 1H, J = 6 Hz, C2′-H), 5.06 (dd, 1H, J = 6, 4 Hz, C3′-H), 4.33 (dd, 1H, J = 10, 4 Hz, C4′-H_A), 4.24 (d, 1H, J = 10 Hz, C4′-H_B), 1.56 (s, 3H, CH_3), 1.39 (s, 3H, CH_3).

5′-Deoxy-2′,3′-O-isopropylidene-5-fluorouridine (1b)—The procedure described above for the synthesis of **1a** was followed for the preparation of **1b** from **5′-dFU** (0.67 g, 2.72 mmol). The yellow solid obtained from chloroform extraction was purified by flash chromatography on silica gel (hexanes/ethyl acetate 1:1) to give **1b** as a white solid (0.70 g, 2.44 mmol, 90%): ^{1}H NMR (500 MHz, $CDCl_3$) δ ppm: 9.42 (s, 1H, NH), 7.39 (d, 1H, J_{HF} = 6 Hz, C6-H), 5.70 (d, 1H, J = 2.5 Hz, C1′-H), 4.9 (dd, 1H, J = 6.5, 2.5 Hz, C2′-H), 4.52 (dd, 1H, J = 6.5, 4.5 Hz, C3′-H), 4.27 (dq, 1H, J = 6.5, 4.5 Hz, C4′-H), 1.59 (s, 3H, CCH_3), 1.43 (d, 3H, J = 6.5 Hz, 4′-CH_3), 1.37 (s, 3H, CCH_3).

2′,3′-O-Isopropylidene-1-(β-D-erythrofuranosyl)-5-fluoroorotic acid ethyl ester (2a)—Freshly prepared LDA (3.2 mmol) was added slowly to a solution of **1a** (0.34 g, 1.23 mmol) in dry THF (10 mL) under argon at −78 °C. The mixture was stirred for 2 h at −78 °C after which ethyl cyanoformate (0.5 mL, 5.06 mmol) was added. After 50 min the reaction was quenched with water (20 mL), stirred for 20 min at room temperature, followed by neutralization of residual HCN by the addition of solid Na_2CO_3 and extraction with ethyl acetate (4 × 30 mL). The combined organic extracts were dried ($MgSO_4$) and the solvent was removed by evaporation under reduced pressure to give a brown oil. Purification by flash chromatography on silica gel (hexanes/ethyl acetate 2:1) gave a yellow solid (0.33 g, 78%) which was recrystallized from hexanes/diethyl ether to give **2a** as a white solid (0.30 g, 70%): mp 159–161 °C. ^{1}H NMR (500 MHz, $CDCl_3$) δ ppm: 8.68 (s, 1H, NH), 5.45 (d, 1H, J = 0.5 Hz, C1′-H), 5.26 (dd, 1H, J = 6.5, 0.5 Hz, C2′-H), 5.09 (m, 1H, C3′-H), 4.52 (q, 2H, J = 7 Hz, $C\underline{H}_2CH_3$), 4.44 (dd, 1H, J = 10, 4 Hz, C4′-H_A), 4.15 (d, 1H, J = 10 Hz, C4′-H_B), 1.53 (s, 3H, CCH_3), 1.45 (t, 3H, J = 7 Hz, $CH_2C\underline{H}_3$), 1.38 (s, 3H, CCH_3). HRMS (ESI): calculated $(M + Na)^+$ $C_{14}H_{17}O_7N_2F_1Na_1$, 367.0912; found, 367.0908.

5′-Deoxy-2′,3′-O-isopropylidene-5-fluororotidine ethyl ester (2b)—The procedure described above for the preparation of **2a** was followed for the preparation of **2b** from **1b** (0.34 g, 1.33 mmol). The crude product, a dark brown oil, was purified by flash chromatography on silica gel (hexanes/ethyl acetate 2:1) to give a yellow solid (0.39 g, 82%). Recrystallization from hexanes/diethyl ether gave **2b** as a white solid (0.36 g, 75%): mp 146–147 °C. ^{1}H NMR (500 MHz, $CDCl_3$) δ ppm: 9.23 (s, 1H, NH), 5.75 (d, 1H, J = 2.5 Hz, C1′-H), 5.17 (dd, 1H, J = 6.5, 2.5 Hz, C2′-H), 4.52 (m, 2H, C3′-H and $C\underline{H}_2CH_3$), 4.42 (m, 1H, $C\underline{H}_2CH_3$), 4.07 (m, 1H, C4′-H), 1.58 (s, 3H, CCH_3), 1.44 (t, 3H, J = 7 Hz, $CH_2C\underline{H}_3$), 1.38 (d, 3H, J = 6.5 Hz, 4′-CH_3), 1.37 (s, 3H, CCH_3). HRMS (ESI): calculated $(M + Na)^+$ $C_{15}H_{19}O_7N_2F_1Na_1$, 381.1069; found, 381.1079.

1-(β-D-Erythrofuranosyl)-5-fluoroorotic acid (FEO)—The hydrolyses of the ethyl ester groups of **2a** and **2b** were carried out in THF containing NaOH. The failure to allow the hydrolysis of **2a** to proceed to completion resulted in poor product yields in the subsequent removal of the isopropylidene group. Therefore, the reaction time was optimized by monitoring a small scale reaction in d_8-THF by ^{1}H NMR, for which the ester hydrolysis was judged to be complete after 2.5 h at room temperature.

2a (132 mg, 0.38 mmol) was dissolved in 2.7 mL of THF and 0.54 mL of 3 M NaOH was added with stirring at room temperature.[22] After 3 h at room temperature the solution was poured into a mixture of 4 mL water and 10 mL of wet Dowex 50WX8-100 (H^+) and stirred for 3 h at room temperature followed by 3 h at 45 °C. The Dowex resin was removed by filtration and washed with water (3 × 20 mL), and the combined aqueous extracts were lyophilized to give **FEO** as a white solid (104 mg, 0.38 mmol, 100 %): mp 212-214 °C. ^{1}H NMR (500 MHz, D_2O) δ ppm: 5.60 (d, 1H, J = 6 Hz, C1′-H), 4.57 (dd, 1H, J = 6, 5 Hz, C2′-H), 4.29 (m, 1H, C3′-H), 4.24 (dd, 1H, J = 10, 3.5 Hz, C4′-H_A), 3.84 (dd, 1H, J = 10 Hz, 1.5 Hz, C4′-H_B). ^{19}F NMR (470 MHz, D_2O) δ ppm: -169.46 (s, 1F, C5-F). HRMS (ESI): calculated $(M + 2Na)^{2+}$ $C_9H_8O_7N_2F_1Na_2$, 321.0105; found, 321.0100.

5′-Deoxy-5-fluoroorotidine (5′-dFO)—The procedure described above for the preparation of **FEO** was followed for the preparation of **5′-dFO** from **2b** (0.040 g, 0.11 mmol), except that removal of the isopropylidene protecting group using Dowex (H^+) employed a 16 h reaction time at 45 °C. This gave **5′-dFO** as a white solid (0.045 g, 0.10 mmol, 90%). ^{1}H NMR (500 MHz, D_2O) δ ppm: 5.33 (d, 1H, J = 2.5 Hz, C1′-H), 4.57 (dd, 1H, J = 6, 2.5 Hz, C2′-H), 3.99 (m, 1H, C3′-H), 3.80 (m, 1H, C4′-H), 1.26 (d, 3H, J = 6.5 Hz, 4′-CH_3). ^{19}F NMR (470 MHz, D_2O) δ ppm: −169.61 (s, 1F, C5-F). HRMS (ESI): calculated $(M - 1)^-$ $C_{10}H_{10}O_7N_2F_1$, 289.0478; found, 289.0478.

Kinetic Studies

Preparation of solutions—Solution pH was determined at 25 °C using an Orion Model 720A pH meter equipped with a Radiometer pHC4006-9 combination electrode that was standardized at pH 7.00 and 10.00 at 25 °C. Stock solutions of **OMP**, **FEO**, **5′-dFO** and orotidine were prepared by dissolution in water followed by adjustment to pH ≈ 7 using 1.0 M NaOH. The stock solution of **5′-dFO** was freed of small amounts of contaminating **5′-dFU** (≤ 1%) by passage over Supelclean™ LC-18 solid phase extraction tubes (3 mL, Supelco), eluting with water. The solutions were stored at −20 °C. The concentrations of **FEO** and **5′-dFO** were determined from the absorbance in 0.1 M HCl at 271 nm using ε = 10,200 M^{-1} cm^{-1} reported for **FOMP**.[4] The concentrations of **OMP** and orotidine were determined from the absorbance in 0.1 M HCl at 267 nm using ε = 9430 M^{-1} cm^{-1} for **OMP** and ε = 9570 M^{-1} cm^{-1} for orotidine.[23]

Stock solutions of sodium phosphite at pH 7.0 (80% dianion) were prepared by addition of a measured amount of 1 M HCl to the sodium salt to give the desired acid/base ratio. MOPS buffers at pH 7.0 (45% free base) or pH 7.1 (50% free base) were prepared by addition of measured amounts of 1 M NaOH and solid NaCl to give the desired acid/base ratio and ionic strength.

Samples of yeast OMPDC that had been stored at −80 °C were defrosted and exhaustively dialyzed at 7 °C against 50 mM MOPS (45% free base) at pH 7.0 and I = 0.14 (NaCl) for the experiments with **FEO** and **5′-dFO**, or 100 mM MOPS (50% free base) at pH 7.1 and I = 0.28 (NaCl) for the experiments with orotidine. The concentration of OMPDC was determined from the absorbance at 280 nm using an extinction coefficient of 29,910 M^{-1} cm^{-1}, calculated using the ProtParam tool available on the ExPASy server.[24]

Standard enzyme assays—The activity of OMPDC in the enzyme stock solutions and in the decarboxylation reaction mixtures was determined by monitoring the decrease in absorbance at 279 nm accompanying the enzyme-catalyzed decarboxylation of **OMP** (Δε = −2400 M^{-1} cm^{-1} at 25 °C).[3,7,8,12] Prior to assay, the stock solutions of OMPDC were diluted with 10 mM MOPS, 50% free base (pH 7.1) containing 100 mM NaCl to give a final concentration of ca. 20 μM OMPDC. Assays in a total volume of 1 mL were conducted in

10 mM MOPS (50% free base) at pH 7.1, 25 °C and I = 0.105 (NaCl), with 40 - 50 μM OMP (25 - 30K_m). Reactions were initiated by the addition of 1 μL of the diluted stock solution of OMPDC or an aliquot of the decarboxylation reaction mixture to give a final enzyme concentration of 20 - 40 nM, and the initial velocity of the ensuing decarboxylation of **OMP** was determined within 1 min.

Yeast OMPDC-catalyzed decarboxylation of FEO—The decarboxylation of **FEO** catalyzed by OMPDC at pH 7.0, 25 °C and I = 0.14 (NaCl) was followed spectrophotometrically by monitoring the decrease in absorbance at 282 nm.[11] Reactions in the absence of phosphite were initiated by the addition of 100 μL of enzyme to give a reaction mixture (1 mL) containing 25 mM MOPS (45% free base, pH 7.0), 0.14 mM **FEO** and 30 μM OMPDC at I = 0.14 (NaCl). Reactions in the presence of phosphite were initiated by the addition of 10 - 100 μL of enzyme to give reaction mixtures (1 mL) at pH 7.0 containing 5 mM MOPS (45% free base), 2 - 36 mM HPO_3^{2-}, 0.14 mM **FEO** and 2.7 - 29 μM OMPDC at I = 0.14 (NaCl). The reactions were monitored for 200 – 800 min (≥ 10 halftimes), after which standard assay (see above) showed that OMPDC maintained full activity towards decarboxylation of **OMP**. In several cases, after completion of the reaction, the enzyme was removed by ultrafiltration (Amicon, 10K MWCO) and the pH of the filtrate was determined. No change in pH was observed during these reactions.

Observed first-order rate constants for enzyme-catalyzed decarboxylation, k_{obs} (s^{-1}), were obtained from the fits of the progress curves to an equation for a single exponential decay.[11] The observed second-order rate constants $(k_{cat}/K_m)_{obs}$ (M^{-1} s^{-1}) were calculated using the relationship $(k_{cat}/K_m)_{obs} = k_{obs}/[E]$.

Yeast OMPDC-catalyzed decarboxylation of 5′-dFO—The decarboxylation of **5′-dFO** catalyzed by OMPDC at pH 7.0, 25 °C and I = 0.14 (NaCl) was followed in a discontinuous assay in which the initial velocity of formation of the product **5′-dFU** was monitored by HPLC analysis with peak detection at 270 nm, as described previously for the decarboxylation of **EO**.[13] Reaction mixtures (200 μL) were prepared by mixing stock solutions of the enzyme in MOPS buffer with stock solutions of MOPS buffer, sodium chloride and, if needed, sodium phosphite (100 mM, 80% dianion), and the reactions were initiated by the addition of an aliquot of the stock solution of **5′-dFO** in water. The reaction conditions in the absence of phosphite dianion were 25 mM MOPS (45% free base, pH 7.0), 0.9 – 9 mM **5′-dFO** and 65 μM OMPDC at I = 0.14 (NaCl). The reaction conditions in the presence of phosphite dianion were 5 mM MOPS (45% free base, pH 7.0), 4 - 32 mM HPO_3^{2-}, 4.4 mM **5′-dFO** and 10 - 50 μM OMPDC at I = 0.14 (NaCl). The reactions were followed for up to 3 hours, during which time there was up to ca. 5% reaction. At various times an aliquot (20 μL) was withdrawn and the reaction was quenched by the addition of 180 μL of a quench solution of formic acid (2.4 mM) containing ca. 60 μM 5-fluorouracil that served as an internal standard. The enzyme was removed by ultrafiltration using an Amicon Ultra device (10K MWCO) that had been prewashed 2 to 3 times with 500 μL of water. Failure to prewash the filtration device resulted in loss of retention and/or erratic HPLC retention times. The filtrate (100 μL) was analyzed by HPLC using a Waters Atlantis dC_{18} 3 Gm column (3.9 × 150 mm) with a linear gradient from 10 mM NH_4OAc pH 4.2 to 60/40 NH_4OAc/MeOH over 10 min, with a flow of 1 mL/min and peak detection at 270 nm. Under these conditions the unreacted **5′-dFO** eluted at 2.5 min, 5-fluorouracil eluted at 4.2 min and the product **5′-dFU** eluted at 11.8 min. The observed HPLC peak area for **5′-dFU** was normalized using the observed peak area for 5-fluorouracil and the standard HPLC peak area for 5-fluorouracil determined by direct HPLC analysis of the formic acid/5-fluorouracil quench solution. This procedure was necessary because there is a small variable dilution of the sample upon its passage through the prewashed filtration device. The concentration of

the product **5′-dFU** in the reaction mixture at time *t*, $[\mathbf{5'\text{-}dFU}]_t$, was then obtained from its normalized HPLC peak area by interpolation of a standard curve that was constructed using 5-fluorouridine. The concentration of 5-fluorouridine in the stock solutions used for this calibration was determined from the absorbance in 0.1 M HCl at 270 nm using $\varepsilon = 9660$ M^{-1} cm^{-1} reported for **FEU**.[17] Periodic standard assay of the reaction mixture using **OMP** as substrate (see above) showed that there was no significant decrease in the activity of OMPDC during these reactions.

Initial velocities of the decarboxylation of **5′-dFO**, v_o ($M\ s^{-1}$), were determined as the slopes of linear plots of $[\mathbf{5'\text{-}dFU}]_t$ against time that covered up to 5% reaction. The observed second-order rate constants $(k_{cat}/K_m)_{obs}$ ($M^{-1}\ s^{-1}$) were determined using the relationship $(k_{cat}/K_m)_{obs} = v_o/[E][\mathbf{5'\text{-}dFO}]_o$, where $[\mathbf{5'\text{-}dFO}]_o$ is the concentration of **5′-dFO** at zero time.

Yeast OMPDC-catalyzed decarboxylation of orotidine—The decarboxylation of orotidine catalyzed by OMPDC at pH 7.1, 25 °C and $I = 0.14$ or 0.21 (NaCl) was followed in a discontinuous assay in which the initial velocity of formation of the product uridine was monitored by HPLC analysis with peak detection at 262 nm.[11] Reaction mixtures (160 μL) were prepared by mixing stock solutions of the enzyme in MOPS buffer with water and, if needed, sodium phosphite (200 μM, 80% dianion), and the reactions were initiated by the addition of an aliquot of the stock solution of orotidine in water. The reaction conditions in the absence of phosphite dianion were 50 mM MOPS (50% free base, pH 7.1), 10.3 mM orotidine and 137 μM OMPDC at $I = 0.14$ (NaCl). The reaction conditions in the presence of phosphite dianion were 25 mM MOPS (50% free base, pH 7.1), 40 mM HPO_3^{2-}, 10.3 mM orotidine and 73 μM OMPDC at $I = 0.21$ (NaCl). The reactions were followed for ca. 30 h, during which time there was ca. 0.5% reaction. At various times an aliquot (20 μL) was withdrawn and the reaction was quenched by the addition of 180 μL of a quench solution of formic acid (6 – 12 mM). The enzyme was removed by ultrafiltration and the sample analyzed by HPLC, as described previously for the decarboxylation of **EO**.[11] The concentration of the product uridine in the reaction mixture at time *t*, $[uridine]_t$, was obtained from the HPLC peak area by interpolation of a standard curve. Periodic standard assay of the reaction mixture using **OMP** as substrate (see above) showed that there was no significant decrease in the activity of OMPDC during these reactions.

Initial velocities of the decarboxylation of orotidine were determined as the slopes of linear plots of $[uridine]_t$ against time that covered up to 0.5% reaction. The observed second-order rate constants $(k_{cat}/K_m)_{obs}$ ($M^{-1}\ s^{-1}$) were determined using the relationship $(k_{cat}/K_m)_{obs} = v_o/[E][orotidine]_o$, where $[orotidine]_o$ is the concentration of orotidine at zero time.

RESULTS

The novel compounds **FEO** and **5′-dFO** were synthesized in good yields using the procedures outlined in Scheme 3. These syntheses represent a novel approach to nucleosides containing an orotate or a 5-fluoroorotate base.

The relatively rapid yeast OMPDC-catalyzed decarboxylation reactions of **FEO** (0.14 mM) to give **FEU** at pH 7.0, 25 °C and $I = 0.14$ (NaCl) in the absence and presence of phosphite dianion were followed spectrophotometrically by monitoring the decrease in absorbance at 282 nm. These reactions were cleanly first-order for the entire reaction time course (≥ 10 halftimes). Observed first-order rate constants for enzyme-catalyzed decarboxylation, $k_{obs}(s^{-1})$, were obtained from the fits of the data to a single exponential.[11] The observed second-order rate constants, $(k_{cat}/K_m)_{obs}$ ($M^{-1}\ s^{-1}$), were calculated using the relationship $(k_{cat}/K_m)_{obs} = k_{obs}/[E]$. The second-order rate constant for the OMPDC-catalyzed

decarboxylation of **FEO** in the absence of phosphite dianion was determined as $(k_{cat}/K_m)_E$ = 10 M^{-1} s^{-1} (Scheme 4).

Figure 1A shows the dependence of the observed second-order rate constant $(k_{cat}/K_m)_{obs}$ for OMPDC-catalyzed decarboxylation of **FEO** on the concentration of added phosphite dianion at pH 7.0, 25 °C and a constant ionic strength of 0.14 (NaCl). There is weak downward curvature at high concentrations of phosphite, which is consistent with partial saturation of the enzyme by HPO_3^{2-} to give the E·HPO_3^{2-} complex (Scheme 4). The solid line shows the nonlinear least squares fit of the data to eq 1, derived for Scheme 4, with $(k_{cat}/K_m)_E$ = 10 M^{-1} s^{-1}, which gave K_d = 0.1 M for binding of phosphite to OMPDC, and $(k_{cat}/K_m)_{E\cdot HPi}$ = 5000 M^{-1} s^{-1} for decarboxylation catalyzed by the phosphite-liganded enzyme E·HPO_3^{2-} (Scheme 4). However, it is also possible that the downward curvature results from a specific salt effect arising from the replacement of Cl^- with HPO_3.[2-7] Therefore, the third-order rate constant for the phosphite-activated reaction of **FEO** was determined as the slope of the linear correlation of the data at $[HPO_3^{2-}] \leq 12$ mM, as $(k_{cat}/K_m)_{E\cdot HPi}/K_d = 4.8 \times 10^4$ M^{-2} s^{-1}. Table 1 reports the rate constants for the unactivated and phosphite-activated reactions of **FEO** that were determined in these experiments.

$$\left(\frac{k_{cat}}{K_m}\right)_{obs} = \left(\frac{K_d}{K_d + \left[HPO_3^{2-}\right]}\right)\left(\frac{k_{cat}}{K_m}\right)_E + \left(\frac{\left[HPO_3^{2-}\right]}{K_d + \left[HPO_3^{2-}\right]}\right)\left(\frac{k_{cat}}{K_m}\right)_{E\cdot HPi} \quad (1)$$

The initial velocities, v_o(M s^{-1}), of the yeast OMPDC-catalyzed decarboxylation of **5′-dFO** (up to 9 mM) at pH 7.0, 25 °C and I = 0.14 (NaCl) were determined by following the formation of up to 5% of the product **5′-dFU** by HPLC. Observed second-order rate constants were determined using the relationship $(k_{cat}/K_m)_{obs} = v_o/[E][\mathbf{5'\text{-}dFO}]_o$, where [**5′-dFO**]$_o$ is the concentration of **5′-dFO** at zero time. The second-order rate constant for the OMPDC-catalyzed decarboxylation of **5′-dFO** in the absence of phosphite dianion was determined as $(k_{cat}/K_m)_E$ = 0.078 M^{-1} s^{-1} (Scheme 4). There was no significant change in the value of $(k_{cat}/K_m)_E$ when the concentration of **5′-dFO** was increased from 0.9 to 9 mM, which shows that there is no significant saturation of OMPDC by 9 mM **5′-dFO**.[11]

Figure 1B shows the dependence of the observed second-order rate constant $(k_{cat}/K_m)_{obs}$ for OMPDC-catalyzed decarboxylation of **5′-dFO** on the concentration of added phosphite dianion at pH 7.0, 25 °C and a constant ionic strength of 0.14 (NaCl). The modest downward curvature is consistent with K_d = 0.050 M (Scheme 4). The third-order rate constant for the phosphite-activated reaction of **5′-dFO** was determined as the slope of the linear correlation of the data at $[HPO_3^{2-}] \leq 8$ mM, as $(k_{cat}/K_m)_{E\cdot HPi}/K_d$ = 16 M^{-2} s^{-1}. Table 1 reports the rate constants for the unactivated and phosphite-activated reactions of **5′-d-FO** that were determined in these experiments.

The second-order rate constant for the yeast OMPDC-catalyzed decarboxylation of orotidine to give uridine at pH 7.1, 25 °C and I = 0.14 (NaCl) in the absence of phosphite dianion was determined by our HPLC assay as $(k_{cat}/K_m)_E = 1.8 \times 10^{-4}$ M^{-1} s^{-1} (Table 1). This is in good agreement with the earlier value of 2×10^{-4} M^{-1} s^{-1} determined under similar conditions by following the release of $^{14}CO_2$ that accompanies the decarboxylation of orotidine labeled at the 6-CO_2^- group.[20] The observed second-order rate constant for the decarboxylation of orotidine in the presence of 40 mM phosphite dianion at pH 7.0, 25 °C and I = 0.21 (NaCl) was determined as $(k_{cat}/K_m)_{obs} = 5.6 \times 10^{-4}$ M^{-1} s^{-1}. This was used to estimate the third-order rate constant for the phosphite-activated reaction of orotidine as $(k_{cat}/K_m)_{E\cdot HPi}/K_d = [(k_{cat}/K_m)_{obs} - (k_{cat}/K_m)_E]/0.04 = 9.3 \times 10^{-3}$ M^{-2} s^{-1} (Table 1).

DISCUSSION

We showed previously that a comparison of the effects of site-directed mutations of OMPDC on the kinetic parameters for decarboxylation of the whole substrate **OMP** and on the decarboxylation of the truncated substrate **EO** activated by the second substrate piece HPO_3^{2-} allows for a clean distinction between the amino acid side chains at OMPDC that interact with the substrate phosphodianion and those that interact with the pyrimidine ring.[12,13] However, the severity of the mutations that can be examined is limited by the low reactivity of the truncated substrate **EO**, for which the second-order rate constant for unactivated decarboxylation catalyzed by wildtype yeast OMPDC is $(k_{cat}/K_m)_E = 0.026\ M^{-1}\ s^{-1}$.[11,13] The desire to characterize an expanded range of mutations prompted us to develop a synthesis of the more reactive 5-fluoro substituted truncated substrate **FEO** (Scheme 3). The high reactivity of this substrate in enzyme-catalyzed decarboxylation has enabled the study of severely impaired site-directed mutants of OMPDC from *Methanothermobacter thermautotrophicus*, which show extremely low activities for the decarboxylation of **EO**.[25]

5-Fluoro Substituent Effects

The addition of a 5-F substituent to **EO** to give **FEO** results in a 390-fold increase in the second-order rate constant for the unactivated yeast OMPDC-catalyzed decarboxylation through a carbanion intermediate (Scheme 1B), from $(k_{cat}/K_m)_E = 0.026\ M^{-1}\ s^{-1}$ for **EO** to $10\ M^{-1}\ s^{-1}$ for **FEO** (Tables 1 and 2). Therefore, the 5-F substituent provides a 3.5 kcal/mol stabilization of the carbanion-like transition state for enzyme-catalyzed decarboxylation (Table 2), which suggests that the *chemical* step of decarboxylation of the enzyme-bound substrate to give the enzyme-bound product **EU** or **FEU** is cleanly rate-determining for these reactions. Similarly, the addition of a 5-F substituent to **UMP** to give **FUMP** results in a 3400-fold increase in the rate constant for the OMPDC-catalyzed C-6 deuterium exchange reaction of the enzyme-bound nucleotide in D_2O (Scheme 2A),[3,5] so that the negative charge in the transition state for formation of the vinyl carbanion intermediate is stabilized by 4.8 kcal/mol by interactions with the 5-F substituent (Table 2). These substituent effects on decarboxylation and deuterium exchange provide a measure of the *change* in the interactions of the reacting center with the 5-F substituent on proceeding from the reactant to the carbanion-like transition state in each case.[26] The effect of a 5-F substituent on the OMPDC-catalyzed *decarboxylation* of **OMP** is ca. 1 kcal/mol smaller than that on the *deuterium exchange* reaction of **UMP** (Table 2). This suggests that the *gain* in the stabilizing interactions of the developing negative charge with the 5-F substituent on proceeding to the transition state for decarboxylation is partly offset by the *loss* of *ground state* stabilizing interactions of the 5-F substituent with the anionic 6-CO_2^- group of the substrate.

The very similar kinetic parameters for the yeast OMPDC-catalyzed decarboxylation reactions of the natural substrate **OMP** ($k_{cat}/K_m = 1.1 \times 10^7\ M^{-1}\ s^{-1}$, $k_{cat} = 15\ s^{-1}$)[7] and of the 5-F substituted substrate **FOMP** ($k_{cat}/K_m = 1.2 \times 10^7\ M^{-1}\ s^{-1}$, $k_{cat} = 95\ s^{-1}$)[27] show that there is little or no effect of a 5-F substituent on the stability of the transition state for decarboxylation of the natural substrate (Scheme 1A). The formation of the Michaelis complex is partly rate-determining for k_{cat}/K_m for turnover of **OMP** by yeast OMPDC,[8] so that these essentially identical large values of k_{cat}/K_m for decarboxylation of **OMP** and the chemically more reactive **FOMP** are consistent with cleanly rate-determining formation of the productive Michaelis complex for **FOMP**, with a second-order rate constant $k_d = k_{cat}/K_m \approx 10^7\ M^{-1}\ s^{-1}$ (Scheme 5). The observed 390-fold effect of a 5-F substituent on the decarboxylation of **EO** can be combined with $k_{cat} = 15\ s^{-1}$ for decarboxylation of enzyme-bound **OMP** to estimate a rate constant of $k_{chem} \approx 6000\ s^{-1}$ for decarboxylation of enzyme-bound **FOMP** to give enzyme-bound **FUMP** (Scheme 5). This is much larger than the *observed* value of $k_{cat} = 95\ s^{-1}$ for **FOMP**,[27] and it is consistent with a change in rate-

determining step for k_{cat} from the chemical step of loss of CO_2 for **OMP** (k_{chem}, Scheme 5), to product release for the much more reactive substrate **FOMP** (k_{off}).[18] These conclusions are supported by the observations of a substantially smaller primary ^{13}C isotope effect on k_{cat}/K_m for the decarboxylation of **FOMP** than for **OMP** labeled at the 6-CO_2^- group,[28] and of larger dependencies on solvent viscosity of the kinetic parameters k_{cat}/K_m and k_{cat} for the decarboxylation of **FOMP** than for **OMP**.[18]

By contrast with the relatively large 390-fold difference in the second-order rate constants for the *unactivated* OMPDC-catalyzed decarboxylation reactions of **EO** and **FEO**, for which the chemical step of the loss of CO_2 from the substrate is cleanly rate-determining, there is only a minimal 4-fold increase in the third-order rate constant $(k_{cat}/K_m)_{E\cdot HPi}/K_d$ for the *phosphite-activated* decarboxylation of **EO** upon the addition of a 5-F substituent to give **FEO** (Table 1). This provides strong evidence that, by analogy with the decarboxylation of **FOMP**, the phosphite-activated decarboxylation of **FEO** is not limited by the chemical step of the loss of CO_2 from the substrate. We conclude that the OMPDC-catalyzed reactions of **FOMP** and of the corresponding substrate pieces **FEO** and HPO_3^{2-} are limited by the formation of the reactive binary E·**FOMP** and ternary E·**FEO**·HPO_3^{2-} complexes, respectively.

Decarboxylation of FEO Limited by a Conformational Change

We have proposed that OMPDC exists in two forms: a predominant *inactive* loop open form, $\mathbf{E_O}$, and a rare *active* loop closed form $\mathbf{E_C}$.[13,17] This conformational change is proposed to result in an environment at the active site that is optimized for catalysis of decarboxylation and deuterium exchange reactions.[13,17] The conversion of $\mathbf{E_O}$ to $\mathbf{E_C}$ involves, at a minimum, closure of the mobile active site loop (loop 7), which sequesters the bound substrate from bulk solvent.[29-32] There is a large difference between the small *observed* binding energy of HPO_3^{2-} at the free ground state enzyme ($K_d \approx 0.1$ M, Scheme 4 and Figure 1) and the much larger *intrinsic* phosphite binding energy of 7.7 kcal/mol for the phosphite-activated reaction of the truncated substrate **EO** (Table 1). This difference is the binding energy that is specifically utilized to stabilize the transition state for enzyme-catalyzed decarboxylation of **EO**.[11,13] We have proposed that the large intrinsic phosphite dianion binding energy is utilized to drive the unfavorable conformational change at OMPDC, and at other enzymes, which converts $\mathbf{E_O}$ to $\mathbf{E_C}$ and activates the enzyme for catalysis.[13,17,33-35] Loop closure and the conformational change is driven by the formation of favorable interactions between phosphite dianion and the closed enzyme $\mathbf{E_C}$, and this dianion binding energy is expressed later at the transition state for decarboxylation.[11,13,33]

Scheme 6 shows our proposed kinetic pathway for the phosphite-activated OMPDC-catalyzed decarboxylation of **FEO**. The binding of **FEO** to the ground state open enzyme $\mathbf{E_O}$ is assumed to precede the binding of HPO_3^{2-}, since dianion binding triggers loop closure over the active site and presumably occludes the binding of the second substrate piece.[29-32] The subsequent binding of phosphite dianion (k_{on}) results in the conformational change and loop closure to give the *productive* ternary Michaelis complex $\mathbf{E_C}$·**FEO**·HPO_3^{2-}. The conclusion that the OMPDC-catalyzed decarboxylation of the substrate pieces **FEO** + HPO_3^{2-} is limited by the formation of the reactive ternary $\mathbf{E_C}$·**FEO**·HPO_3^{2-} complex (see above) shows that the *chemical* step for decarboxylation of **FEO** is faster than release of phosphite dianion from the enzyme, $k_{chem} > k_{off}$ (Scheme 6), so that the binding of phosphite is essentially irreversible. However, this must be reconciled with the observed *low* affinity of OMPDC for phosphite dianion, $K_d = k_{off}/k_{on} \approx 0.1$ M, because weak binding is usually associated with fast ligand release to solution, which would tend to strongly favor a rate-determining chemical step.

Scheme 6 shows that the overall binding of phosphite involves at least two steps: the initial encounter-limited formation of a *weak* complex of HPO_3^{2-} with the **E_O·FEO** complex (k_d), followed by a conformational change (k_c) to give the productive ternary Michaelis complex **E_C·FEO**·HPO_3^{2-}. The first-order rate constant for decarboxylation of enzyme-bound **FEO** at the ternary complex can be estimated as $k_{chem} \leq 6000\ s^{-1}$, with the assumption that the decarboxylation of **FEO** should be no faster than the decarboxylation of enzyme-bound **FOMP** (see above). Therefore, the requirement $k_{chem} > k_{off}$ and the value of $K_d \approx 0.1$ M (we assume that phosphite binds to **E_O** and **E_O·FEO** with similar affinities), give $k_{on} \leq 6 \times 10^4\ M^{-1}\ s^{-1}$ for binding of phosphite dianion to **E_O·FEO** to give the reactive **E_C·FEO**·HPO_3^{2-} complex. This *slow* irreversible formation of the reactive ternary complex strongly suggests that the binding of phosphite is limited *not* by diffusional encounter ($k_d \approx 10^7\ M^{-1}\ s^{-1}$), but rather by the conformational change that results in closure of the loop over the active site (k_c, Scheme 6).

The conclusion that the phosphite-activated decarboxylation of **FEO** is limited by the conformational change that converts the inactive enzyme at the ternary **E_O·FEO**·HPO_3^{2-} complex to the active enzyme at the **E_C·FEO**·HPO_3^{2-} complex contrasts the observed encounter-limited formation of the reactive **E_C·FOMP** complex with $k_{cat}/K_m = k_d \approx 1 \times 10^7\ M^{-1}\ s^{-1}$ (Scheme 5). These results suggest that there is a larger barrier to loop motion and the conformational change at the **E_O·FEO**·HPO_3^{2-} complex than at the physiological **E_O·FOMP** complex, resulting in a change in rate-limiting step for the overall decarboxylation from k_d for the reaction of **FOMP** (Scheme 5) to k_c for the *phosphite-activated* reaction of **FEO** (Scheme 6). We suggest that the slower closure of the loop at **E_O·FEO**·HPO_3^{2-} than at **E_O·FOMP** results from a higher entropy of activation for the former process, arising from a greater requirement for "freezing" the conformation of weakly bound HPO_3^{2-} at **E_O·FEO**·HPO_3^{2-} on proceeding to the tighter **E_C·FEO**·HPO_3^{2-} complex.

4′-Substituent Effects

Table 3 summarizes the effects of 4′-$CH_2OPO_3^{2-}$, 4′-CH_2OH and 4′-CH_3 substituents on the unactivated and the phosphite-activated OMPDC-catalyzed decarboxylation reactions of the truncated substrates **EO** and/or **FEO**.

The large 4×10^8-fold difference in the second-order rate constants for OMPDC-catalyzed decarboxylation of the natural substrate **OMP** ($k_{cat}/K_m = 1.1 \times 10^7\ M^{-1}\ s^{-1}$) [7] and the truncated substrate **EO** [$(k_{cat}/K_m)_E = 0.026\ M^{-1}\ s^{-1}$][13] shows that the 4′-$CH_2OPO_3^{2-}$ substituent stabilizes the transition state for decarboxylation by 11.7 kcal/mol.[7,11,13] However, this large intrinsic phosphate binding energy[36] is not fully expressed for the decarboxylation of **FOMP**. Here the *encounter-limited* decarboxylation of **FOMP** (see above) results in only a 1×10^6-fold difference in the second-order rate constants for the OMPDC-catalyzed decarboxylation reactions of **FOMP** and **FEO**. The observed transition state stabilization from the 4′-$CH_2OPO_3^{2-}$ group of **FOMP** is only 8.3 kcal/mol, which suggests that the barrier to the decarboxylation of **FOMP** is ca. 3.4 kcal/mol lower than that expected if the chemical step were rate-determining. This is consistent with a rate constant ratio of $k_{chem}/k_{-d} \approx 300$ for partitioning of enzyme-bound **FOMP** between decarboxylation and release to solution (Scheme 5). The dependence of k_{cat}/K_m for the decarboxylation of **OMP** on solvent viscosity is consistent with a partitioning ratio of $k_{chem}/k_{-d} \approx 0.6$ for the reaction of **OMP**,[18] which is similar to the reported commitment to catalysis of $k_{cat}/k_{-d} = 0.3$.[8] If there is little or no effect of a 5-F substituent on the rate constant k_{-d} for release of the enzyme-bound nucleotide to solution, these observations suggest that there is a ca. 500-fold effect of a 5-F substituent on k_{chem} for decarboxylation of the enzyme-bound nucleotide (Scheme 5). This is very similar to the 400-fold effect of a 5-F substituent on

decarboxylation determined directly from the unactivated OMPDC-catalyzed decarboxylation reactions of **FEO** and **EO**, for which the chemical step is cleaning rate-limiting (Table 2).

We expected that the phosphodianion binding pocket of OMPDC would easily accommodate the 4′-CH_3 group of **5′-dFO** at the transition state for enzyme-catalyzed decarboxylation, because the enzyme has evolved to accommodate the presumably even larger 4′-$CH_2OPO_3^{2-}$ group of **OMP**. We were therefore very surprised to find that the addition of a 4′-CH_3 group to **FEO** to give **5′-dFO** results in a substantial 130-fold decrease in the rate constant for the unactivated decarboxylation and a 2.9 kcal/mol destabilization of the transition state (Table 3). There is an even larger 3000-fold effect (4.7 kcal/mol transition state destabilization) of the addition of a 4′-CH_3 group to **FEO** to give **5′-dFO** on the third-order rate for the phosphite-activated reactions of these substrates. Therefore, not surprisingly, the steric effect of the 4′-CH_3 group on decarboxylation at the ternary **E**·**5′-dFO**·HPO_3^{2-} complex is larger than that at the binary **E**·**5′-dFO** complex.

Interestingly, the 4′-CH_2OH group of orotidine results in the *same* 2.9 kcal/mol destabilization of the transition state for decarboxylation observed for the 4′-CH_3 group of **5′- dFO**, and there are similar stabilizations of the transition states for these reactions by the binding of phosphite dianion of 2.3 and 3.2 kcal/mol, respectively (Table 1). This suggests that there is little contribution of the terminal 5′-OH group of orotidine to the stability of the transition state for decarboxylation. By contrast, the 4′-CH_2OH group of orotidine results in a very large 8.3 kcal/mol destabilization of the transition state for phosphite-activated decarboxylation, exceeding the destabilization observed for the 4′-CH_3 group of **5′-dFO** by 3.6 kcal/mol (Table 3). The destabilization of the transition state for the latter is masked because the reactivity of the parent two-part substrate **FEO** + phosphite is attenuated by the rate-limiting conformational change (see above).

These surprisingly large 4′-CH_3 and 4′-CH_2OH substituent effects on the decarboxylation reactions of **FEO** and **EO** are consistent with destabilization of the transition state for decarboxylation by steric effects of these groups that disrupt the required precise positioning of the peptide backbone and amino acid side chains at the reactive closed form of OMPDC. This is consistent with our earlier proposal that the binding energy of the substrate phosphodianion group is utilized to stabilize a rare active closed form of OMPDC that is required for the decarboxylation of both whole and truncated substrates.[13,17,25,35]

Acknowledgments

We thank Professor Steven Diver for helpful discussions regarding the synthesis of **FEO** and **5′-dFO**.

Abbreviations

OMPDC	orotidine 5′-monophosphate decarboxylase
OMP	orotidine 5′-monophosphate
UMP	uridine 5′-monophosphate
FOMP	5-fluoroorotidine 5′-monophosphate
FUMP	5-fluorouridine 5′-monophosphate
EO	1-(β-D-erythrofuranosyl)orotic acid
EU	1-(β-D-erythrofuranosyl)uracil

FEO	1-(β-D-erythrofuranosyl)-5-fluoroorotic acid
FEU	1-(β-D-erythrofuranosyl)-5-fluorouracil
5′-dFO	5′-deoxy-5-fluoroorotidine
5′-dFU	5′-deoxy-5-fluorouridine
LDA	lithium diisopropylamide
BuLi	butyllithium
THF	tetrahydrofuran
MOPS	3-(N-morpholino)propanesulfonic acid
NMR	nuclear magnetic resonance

REFERENCES

1. Radzicka A, Wolfenden R. A proficient enzyme. Science. 1995; 267:90–93. [PubMed: 7809611]
2. Miller BG, Wolfenden R. Catalytic proficiency: the unusual case of OMP decarboxylase. Annu. Rev. Biochem. 2002; 71:847–885. [PubMed: 12045113]
3. Tsang W-Y, Wood BM, Wong FM, Wu W, Gerlt JA, Amyes TL, Richard JP. Proton Transfer from C-6 of Uridine 5′-Monophosphate Catalyzed by Orotidine 5′-Monophosphate Decarboxylase: Formation and Stability of a Vinyl Carbanion Intermediate and the Effect of a 5-Fluoro Substituent. J. Am. Chem. Soc. 2012; 134:14580–14594. [PubMed: 22812629]
4. Toth K, Amyes TL, Wood BM, Chan K, Gerlt JA, Richard JP. Product Deuterium Isotope Effects for Orotidine 5′-Monophosphate Decarboxylase: Effect of Changing Substrate and Enzyme Structure on the Partitioning of the Vinyl Carbanion Reaction Intermediate. J. Am. Chem. Soc. 2010; 132:7018–7024. [PubMed: 20441167]
5. Amyes TL, Wood BM, Chan K, Gerlt JA, Richard JP. Formation and Stability of a Vinyl Carbanion at the Active Site of Orotidine 5′-Monophosphate Decarboxylase: pK_a of the C-6 Proton of Enzyme-Bound UMP. J. Am. Chem. Soc. 2008; 130:1574–1575. [PubMed: 18186641]
6. Toth K, Amyes TL, Wood BM, Chan K, Gerlt JA, Richard JP. Product Deuterium Isotope Effect for Orotidine 5′-Monophosphate Decarboxylase: Evidence for the Existence of a Short-Lived Carbanion Intermediate. J. Am. Chem. Soc. 2007; 129:12946–12947. [PubMed: 17918849]
7. Toth K, Amyes TL, Wood BM, Chan KK, Gerlt JA, Richard JP. An Examination of the Relationship between Active Site Loop Size and Thermodynamic Activation Parameters for Orotidine 5′-Monophosphate Decarboxylase from Mesophilic and Thermophilic Organisms. Biochemistry. 2009; 48:8006–8013. [PubMed: 19618917]
8. Porter DJT, Short SA. Yeast Orotidine-5′-Phosphate Decarboxylase: Steady-State and Pre-Steady-State Analysis of the Kinetic Mechanism of Substrate Decarboxylation. Biochemistry. 2000; 39:11788–11800. [PubMed: 10995247]
9. Jencks WP. Binding Energy, Specificity and Enzymic Catalysis: The Circe Effect. Adv. Enzymol. Relat. Areas Mol. Biol. 1975; 43:219–410. [PubMed: 892]
10. Amyes TL, Richard JP. Specificity in Transition State Binding: The Pauling Model Revisited. Biochemistry. 2012; 51 in press.
11. Amyes TL, Richard JP, Tait JJ. Activation of orotidine 5′-monophosphate decarboxylase by phosphite dianion: The whole substrate is the sum of two parts. J. Am. Chem. Soc. 2005; 127:15708–15709. [PubMed: 16277505]
12. Barnett SA, Amyes TL, Wood BM, Gerlt JA, Richard JP. Dissecting the Total Transition State Stabilization Provided by Amino Acid Side Chains at Orotidine 5′-Monophosphate Decarboxylase: A Two-Part Substrate Approach. Biochemistry. 2008; 47:7785–7787. [PubMed: 18598058]

13. Amyes TL, Ming SA, Goldman LM, Wood BM, Desai BJ, Gerlt JA, Richard JP. Orotidine 5′-monophosphate decarboxylase: Transition state stabilization from remote protein-phosphodianion interactions. Biochemistry. 2012; 51:4630–4632. [PubMed: 22620855]
14. Chan KK, Wood BM, Fedorov AA, Fedorov EV, Imker HJ, Amyes TL, Richard JP, Almo SC, Gerlt JA. Mechanism of the Orotidine 5′-Monophosphate Decarboxylase-Catalyzed Reaction: Evidence for Substrate Destabilization. Biochemistry. 2009; 48:5518–5531. [PubMed: 19435314]
15. Amyes TL, Richard JP. Determination of the pK_a of Ethyl Acetate: Brønsted Correlation for Deprotonation of a Simple Oxygen Ester in Aqueous Solution. J. Am. Chem. Soc. 1996; 118:3129–3141.
16. Richard JP, Amyes TL. Proton transfer at carbon. Curr. Opin. Chem. Biol. 2001; 5:626–633. [PubMed: 11738171]
17. Goryanova B, Amyes TL, Gerlt JA, Richard JP. OMP Decarboxylase: Phosphodianion Binding Energy Is Used To Stabilize a Vinyl Carbanion Intermediate. J. Am. Chem. Soc. 2011; 133:6545–6548. [PubMed: 21486036]
18. Wood BM, Chan KK, Amyes TL, Richard JP, Gerlt JA. Mechanism of the Orotidine 5′-Monophosphate Decarboxylase-Catalyzed Reaction: Effect of Solvent Viscosity on Kinetic Constants. Biochemistry. 2009; 48:5510–5517. [PubMed: 19435313]
19. Barnett SA, Amyes TL, McKay Wood B, Gerlt JA, Richard JP. Activation of R235A Mutant Orotidine 5′-Monophosphate Decarboxylase by the Guanidinium Cation: Effective Molarity of the Cationic Side Chain of Arg-235. Biochemistry. 2010; 49:824–826. [PubMed: 20050635]
20. Sievers A, Wolfenden R. The effective molarity of the substrate phosphoryl group in the transition state for yeast OMP decarboxylase. Bioorg. Chem. 2005; 33:45–52. [PubMed: 15668182]
21. Bello AM, Konforte D, Poduch E, Furlonger C, Wei L, Liu Y, Lewis M, Pai EF, Paige CJ, Kotra LP. Structure-activity relationships of orotidine-5′-monophosphate decarboxylase inhibitors as anticancer agents. J. Med. Chem. 2009; 52:1648–1658. [PubMed: 19260677]
22. Wang Y, Burton DJ. A Facile, General Synthesis of 3,4-Difluoro-6-substituted-2-pyrones. J. Org. Chem. 2006; 71:3859–3862. [PubMed: 16674060]
23. Moffatt JG. The synthesis of orotidine 5′-phosphate. J. Am. Chem. Soc. 1963; 85:1118–1123.
24. Gasteiger E, Gattiker A, Hoogland C, Ivanyi I, Appel RD, Bairoch A. ExPASy: The proteomics server for in-depth protein knowledge and analysis. Nucleic Acids Res. 2003; 31:3784–3788. [PubMed: 12824418]
25. Desai BJ, Wood BM, Fedorov AA, Fedorov EV, Goryanova B, Amyes TL, Richard JP, Almo SC, Gerlt JA. Conformational changes in orotidine 5′-monophosphate decarboxylase: A structure-based explanation for how the 5′-phosphate group activates the enzyme. Biochemistry. 2012; 51:8665–8678. [PubMed: 23030629]
26. Hupe DJ, Jencks WP. Nonlinear Structure-Reactivity Correlations. Acyl Transfer between Sulfur and Oxygen Nucleophiles. J. Am. Chem. Soc. 1977; 99:451–464.
27. Barnett, SA.; University at Buffalo. Ph.D. Thesis. Buffalo, New York: 2009. Studies on the Mechanism of Action of Orotidine 5′-Monophosphate Decarboxylase.
28. Van Vleet JL, Reinhardt LA, Miller BG, Sievers A, Cleland WW. Carbon isotope effect study on orotidine 5′-monophosphate decarboxylase: support for an anionic intermediate. Biochemistry. 2008; 47:798–803. [PubMed: 18081312]
29. Wu N, Mo Y, Gao J, Pai EF. Electrostatic stress in catalysis: structure and mechanism of the enzyme orotidine monophosphate decarboxylase. Proc. Natl. Acad. Sci. U. S. A. 2000; 97:2017–2022. [PubMed: 10681441]
30. Miller BG, Hassell AM, Wolfenden R, Milburn MV, Short SA. Anatomy of a proficient enzyme: the structure of orotidine 5′-monophosphate decarboxylase in the presence and absence of a potential transition state analog. Proc. Natl. Acad. Sci. U. S. A. 2000; 97:2011–2016. [PubMed: 10681417]
31. Harris P, Poulsen J-CN, Jensen KF, Larsen S. Structural Basis for the Catalytic Mechanism of a Proficient Enzyme: Orotidine 5′-Monophosphate Decarboxylase. Biochemistry. 2000; 39:4217–4224. [PubMed: 10757968]

32. Begley TP, Appleby TC, Ealick SE. The structural basis for the remarkable catalytic proficiency of orotidine 5′-monophosphate decarboxylase. Curr. Opin. Struct. Biol. 2000; 10:711–718. [PubMed: 11114509]

33. Richard JP. A Paradigm for Enzyme-Catalyzed Proton Transfer at Carbon: Triosephosphate Isomerase. Biochemistry. 2012; 51:2652–2661. [PubMed: 22409228]

34. Malabanan MM, Amyes TL, Richard JP. A role for flexible loops in enzyme catalysis. Curr. Opin. Struct. Biol. 2010; 20:702–710. [PubMed: 20951028]

35. Tsang W-Y, Amyes TL, Richard JP. A Substrate in Pieces: Allosteric Activation of Glycerol 3-Phosphate Dehydrogenase (NAD+) by Phosphite Dianion. Biochemistry. 2008; 47:4575–4582. [PubMed: 18376850]

36. Morrow JR, Amyes TL, Richard JP. Phosphate Binding Energy and Catalysis by Small and Large Molecules. Acc. Chem. Res. 2008; 41:539–548. [PubMed: 18293941]

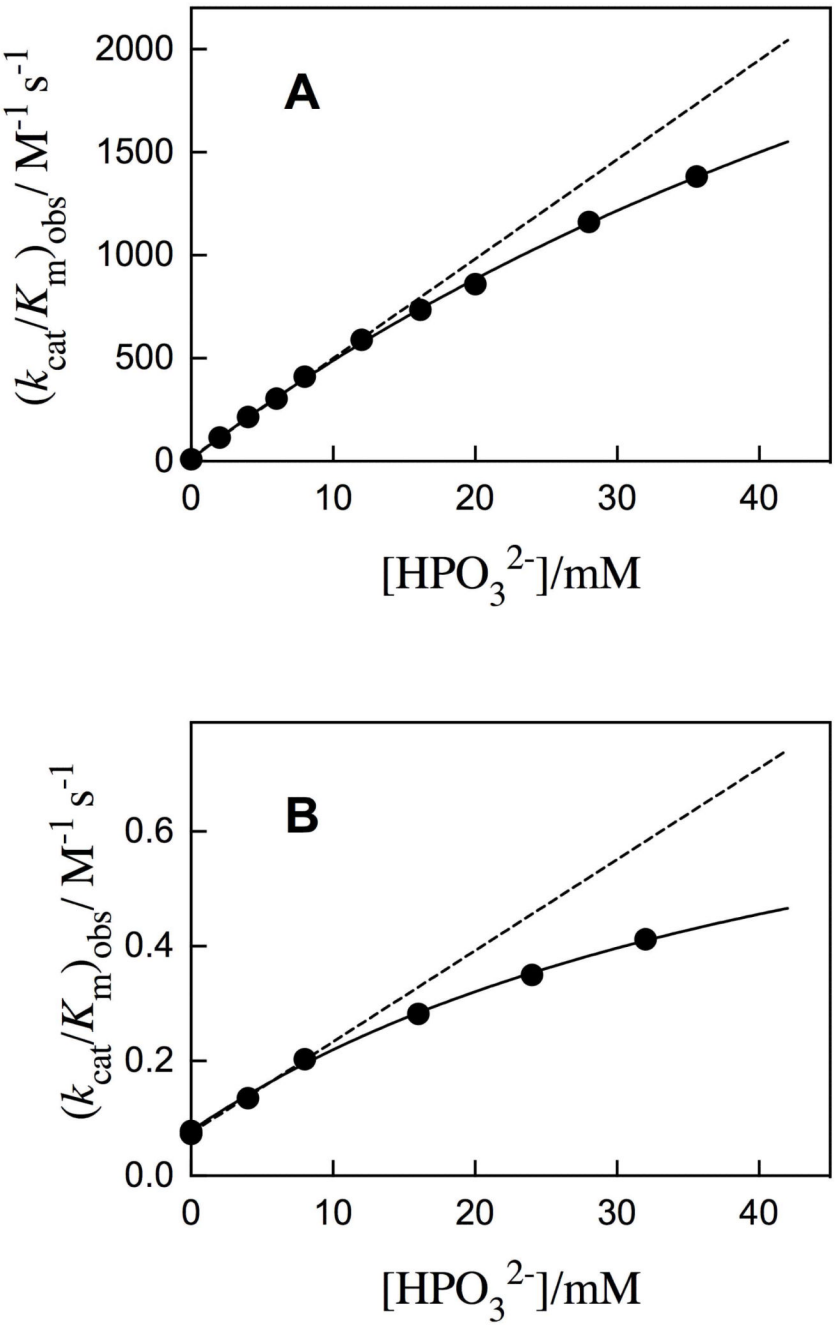

Figure 1.

Dependence of the observed second-order rate constant for the yeast OMPDC-catalyzed decarboxylation of truncated substrates on the concentration of added phosphite dianion at pH 7.0, 25 °C and I = 0.14 (NaCl). A. Decarboxylation of **FEO**. The solid line shows the fit of the data to eq 1, derived for Scheme 4, with $(k_{cat}/K_m)_E$ = 10 M^{-1} s^{-1} and K_d = 0.1 M. The dashed line is the linear correlation at $[HPO_3^{2-}] \leq 12$ mM, the slope of which gives the third-order rate constant $(k_{cat}/K_m)_{E\cdot HPi}/K_d = 4.8 \times 10^4$ M^{-2} s^{-1}. B. Decarboxylation of **5′-dFO**. The solid line shows the fit of the data to eq 1 with $(k_{cat}/K_m)_E$ = 0.078 M^{-1} s^{-1} and K_d = 0.05 M. The dashed line is the linear correlation at $[HPO_3^{2-}] \leq 8$ mM, the slope of which gives the third-order rate constant $(k_{cat}/K_m)_{E\cdot HPi}/K_d$ = 16 M^{-2} s^{-1}.

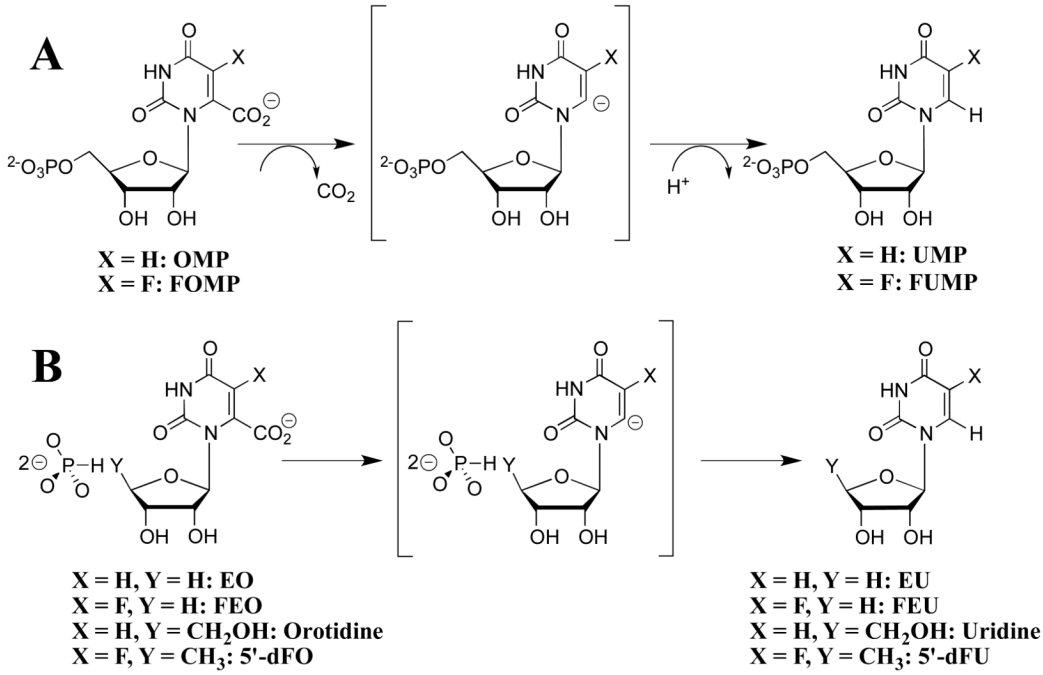

Scheme 1.

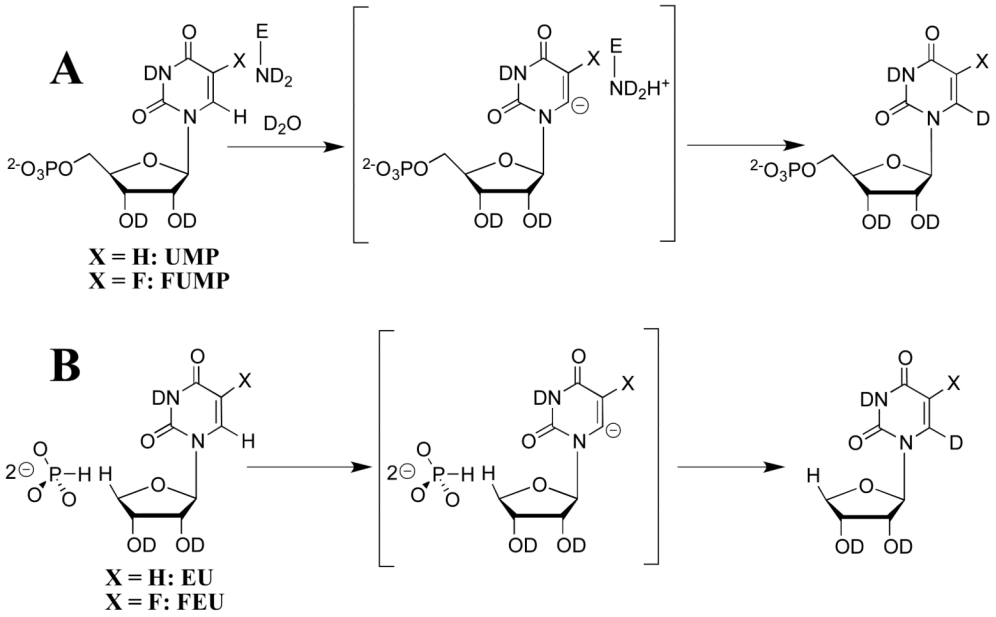

Scheme 2.

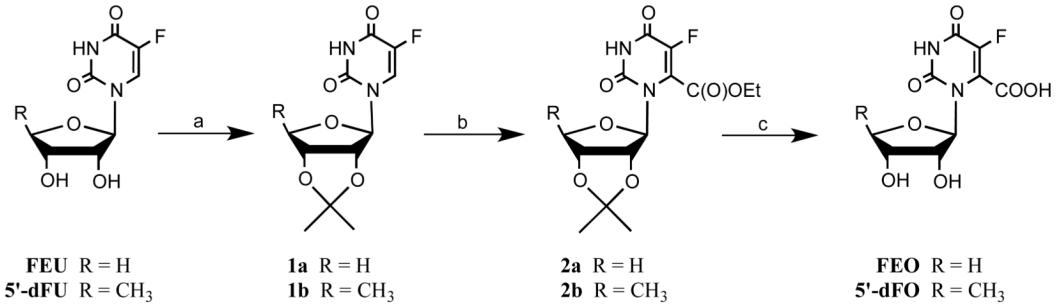

FEU R = H
5'-dFU R = CH_3

1a R = H
1b R = CH_3

2a R = H
2b R = CH_3

FEO R = H
5'-dFO R = CH_3

Scheme 3.

Reagents and conditions: (a) H_2SO_4, acetone, room temperature, 1.5 h, ~ 90%; (b) (i) LDA, THF, −78 °C, 2 h; (ii) EtOC(O)CN, THF, −78 °C, 50 min, 70–75%; (c) (i) NaOH/THF, room temperature, 3 h; (ii) Dowex 50WX8-100 (H^+), H_2O, 45 °C, 90–100%.

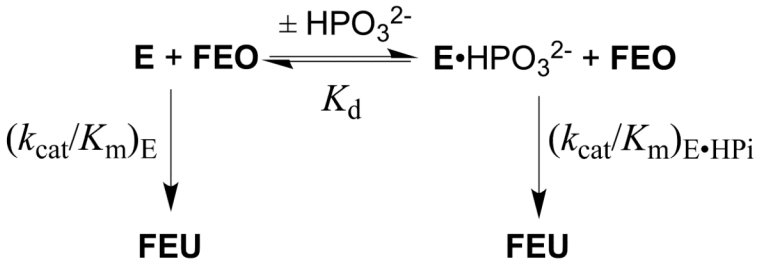

Scheme 4.

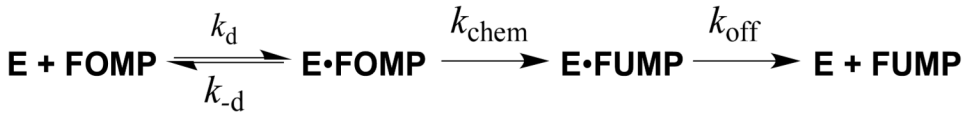

Scheme 5.

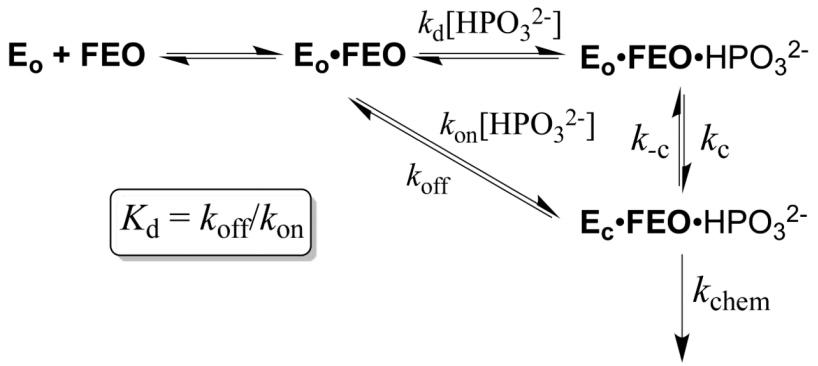

Scheme 6.

Table 1

Kinetic parameters for the decarboxylation of truncated substrates catalyzed by yeast OMPDC and for activation by phosphite dianion at 25 °C.[a]

	EO	FEO	Orotidine	5′-dFO
$(k_{cat}/K_m)_E$[b] (M^{-1} s^{-1})	0.026[c]	10	1.8×10^{-4}[d]	0.078
$(k_{cat}/K_m)_{E\cdot HPi}/K_d$[e] ($M^{-2}$ s^{-1})	1.2×10^4[f]	4.8×10^4	9.3×10^{-3}[g]	16
Activation by 1 M HPO_3^{2-}	5×10^5-fold	5×10^3-fold	50-fold	200-fold
Intrinsic Phosphite Binding Energy (kcal/mol)	7.7	5.0	2.3	3.2

[a] At pH 7.0 and I = 0.14 (NaCl), unless noted otherwise.

[b] Second-order rate constant for the unactivated OMPDC-catalyzed decarboxylation of the truncated substrate in the absence of phosphite. The estimated error is ± 10%.

[c] Data from Ref. 13.

[d] At pH 7.1.

[e] Third-order rate constant for the phosphite-activated OMPDC-catalyzed decarboxylation of the truncated substrate. The estimated error is ± 20%.

[f] Data from Ref. 11.

[g] At pH 7.1 and I = 0.21 (NaCl).

Table 2

Effect of a 5-fluoro substituent on decarboxylation and C-6 deuterium exchange reactions catalyzed by yeast OMPDC at 25 °C.

Substrate	Reaction	Rate Constant	Effect of 5-F Substituent	ΔΔG‡ (kcal/mol)
OMP	Decarboxylation	k_{cat}/K_m (M^{-1} s^{-1})	None [a]	0
EO	Decarboxylation	$(k_{cat}/K_m)_E$ (M^{-1} s^{-1})	+ 390-fold [b]	−3.5
EO + HPO_3^{2-}	Decarboxylation	$(k_{cat}/K_m)_{E\cdot HPi}/K_d$ (M^{-2} s^{-1})	+ 4-fold b	−0.8
UMP	Exchange	k_{ex} (s^{-1})	+ 3400-fold [c]	−4.8

[a]Calculated from the values of k_{cat}/K_m for the decarboxylation reactions of OMP (1.1×10^7 M^{-1} s^{-1}, Ref. 7) and **FOMP** (1.2×10^7 M^{-1} s^{-1}, Ref. 27) at pH 7.1 and I = 0.105 (NaCl).

[b]Calculated from the data in Table 1 for the unactivated and phosphite-activated reactions of **EO** and **FEO** at pH 7.0 and I = 0.14 (NaCl).

[c]Calculated from the pD-independent values of k_{ex} for the C-6 deuterium exchange reactions of enzyme-bound **FUMP** (0.041 s^{-1}) and UMP (1.2×10^{-5} s^{-1}) in D_2O at I = 0.10 (NaCl) (data from Ref. 3).

Table 3

Effect of 4′-substituents on the decarboxylation reactions of the truncated substrates **EO** and **FEO** catalyzed by yeast OMPDC at 25 °C.

Substrate	4′-Substituent	Effect of 4′-Substituent	ΔΔG‡ (kcal/mol)
EO	$CH2OPO_3^{2-}$	+ 4.2×10^8-fold [a]	−11.7
FEO	$CH_2OPO_3^{2-}$	+ 1.2×10^6-fold [a]	−8.3
EO	CH_2OH	−140-fold [b]	+2.9
EO + HPO_3^{2-}	CH_2OH	-1.3×10^6-fold [c]	+8.3
FEO	CH_3	−130-fold [b]	+2.9
FEO + HPO_3^{2-}	CH_3	−3000-fold [c]	+4.7

[a]Calculated from the values of k_{cat}/K_m for the decarboxylation of OMP (1.1×10^7 M^{-1} s^{-1}, Ref. 7) and FOMP (1.2×10^7 M^{-1} s^{-1}, Ref. 27) at pH 7.1 and I = 0.105 (NaCl) and the values of (k_{cat}/K_m)E in Table 1 for the decarboxylation of EO and FEO at pH 7.0 and I = 0.14 (NaCl).

[b]Calculated from the values of (k_{cat}/K_m)E in Table 1 for the unactivated decarboxylation reactions of EO, orotidine, **FEO**, and **5′-dFO** at pH 7.0 or pH 7.1 (for orotidine) and I = 0.14 (NaCl).

[c]Calculated from the values of $(k_{cat}/K_m)_{E\cdot Hpi}/K_d$ in Table 1 for the phosphite-activated decarboxylation reactions of **EO**, **FEO**, and 5′**-dFO** at pH 7.0 and I = 0.14 (NaCl) and the reaction of orotidine at pH 7.1 and I = 0.21 (NaCl).